

DIVERSITY OF DECLINE-RATE-CORRECTED TYPE Ia SUPERNOVA RISE TIMES: ONE MODE OR TWO?

MARK STROVINK

Physics Department and E. O. Lawrence Berkeley National Laboratory
University of California, Berkeley, CA 94720

Draft 2007 4 May

ABSTRACT

B-band light-curve rise times for eight unusually well-observed nearby Type Ia supernovae (SNe) are fitted by a newly developed template-building algorithm, using light-curve functions that are smooth, flexible, and free of potential bias from externally derived templates and other prior assumptions. From the available literature, photometric *BVRI* data collected over many months, including the earliest points, are reconciled, combined, and fitted to a unique time of explosion for each SN. On average, after they are corrected for light-curve decline rate, three SNe rise in 18.81 ± 0.36 days, while five SNe rise in 16.64 ± 0.21 days. If all eight SNe are sampled from a single parent population (a hypothesis not favored by statistical tests), the rms intrinsic scatter of the decline-rate-corrected SN rise time is $0.96^{+0.52}_{-0.25}$ days – a first measurement of this dispersion. The corresponding global mean rise time is 17.44 ± 0.39 days, where the uncertainty is dominated by intrinsic variance. This value is ≈ 2 days shorter than two published averages that nominally are twice as precise, though also based on small samples. When comparing high-*z* to low-*z* SN luminosities for determining cosmological parameters, bias can be introduced by use of a light-curve template with an unrealistic rise time. If the period over which light curves are sampled depends on *z* in a manner typical of current search and measurement strategies, a two-day discrepancy in template rise time can bias the luminosity comparison by ≈ 0.03 magnitudes.

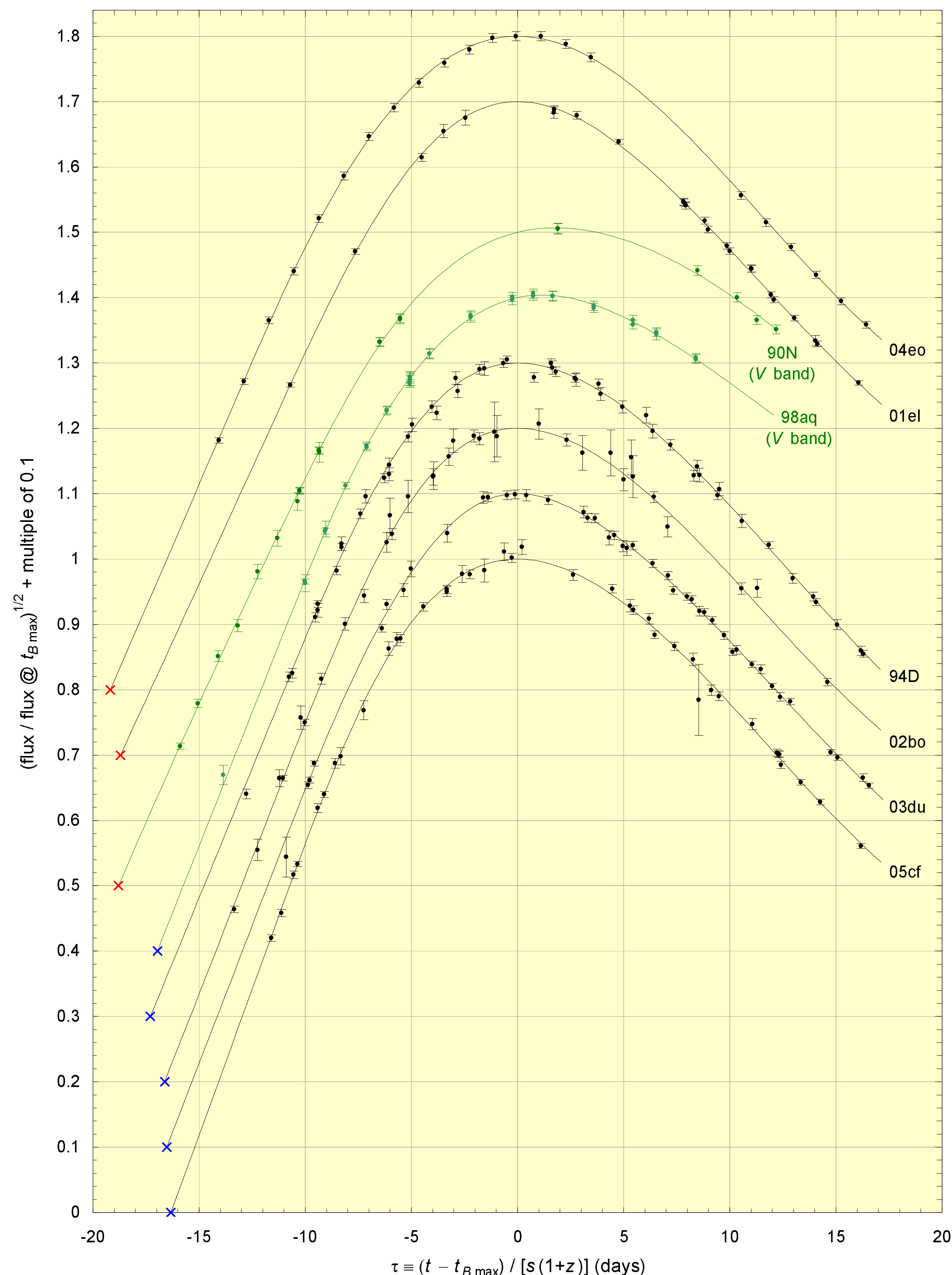


FIG. 1.— Representative AQUAA light-curve fits. The abscissa τ is the SN phase relative to $t_{B\max}$, diluted by a factor s so that $\Delta m_{15} \equiv 1^{st}$ in *B* band. The ordinate is the square root of the flux relative to its value at $\tau = 0$, offset by a multiple of 0.1. *B*-band data are shown for SN 2005cf, SN 2003du, SN 2002bo, SN 1994D, SN 2001el, and SN 2004eo; *V*-band data are shown for SN 1998aq and SN 1990N. The intersections of the fitted curves with zero flux, shown by “x”, are the best-fitted *s*-corrected times of explosion.

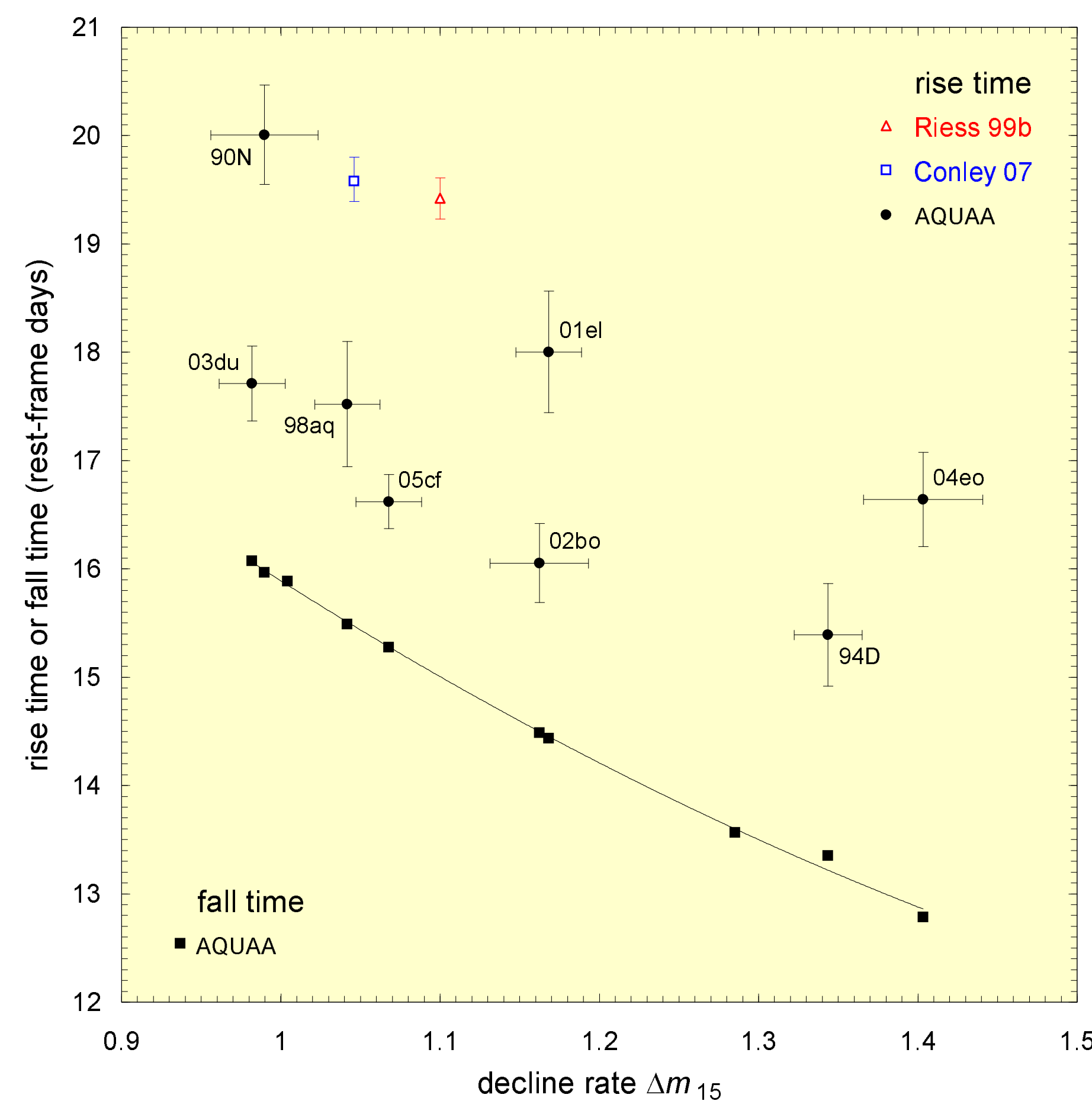


FIG. 2.— Fitted rise time or fall time (defined in the text) vs. decline rate Δm_{15} . Filled circles show the AQUAA fitted rise times for individual SNe. For each SN, both statistical and systematic uncertainties are included in its horizontal and vertical error, which are positively correlated. Filled squares show the AQUAA fitted fall times for the same SNe (plus two others with scant pre-maximum data). The quadratic curve is drawn to guide the eye. Open symbols show the results of previous rise time fits by Riess99b (triangle) and Con07 (square) to ensembles of stretch-corrected low-*z* SNe.

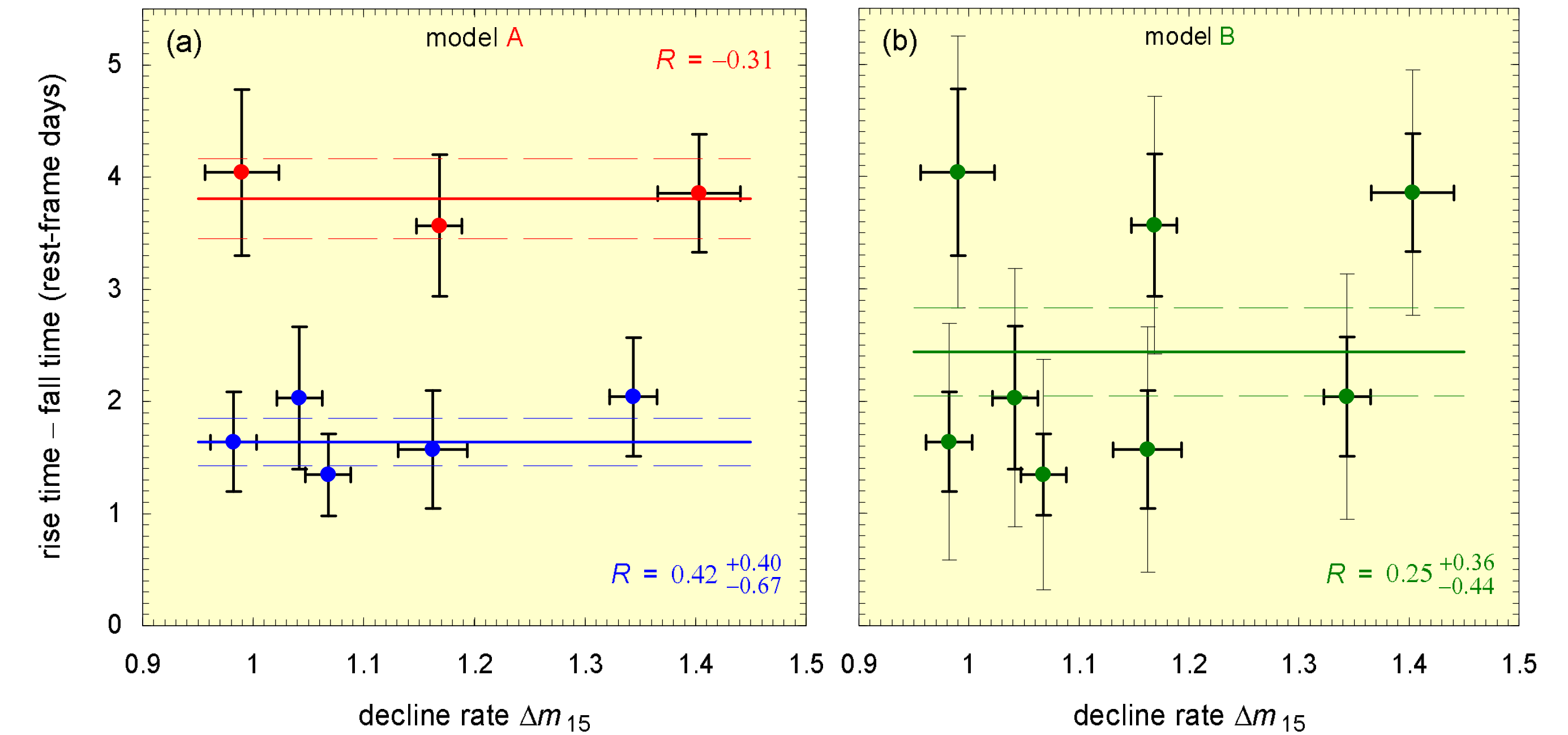


FIG. 3.— (a) Difference between the rise time and fall time shown in Fig. 2 vs. decline rate Δm_{15} . The error bars represent the combined statistical and systematic uncertainties. Horizontal lines depict the ordinates best fitted to the slowest-rising three SNe (top) and to the fastest-rising five SNe (bottom) with their one-standard-deviation uncertainties. The exhibited Pearson coefficients R show that the abscissa and ordinate are not significantly correlated for either set of points. (b) Same as (a) except that a single ordinate is fit to all eight SNe using the outer error bars, which include a 0.96-day intrinsic rise-time variation added in quadrature.

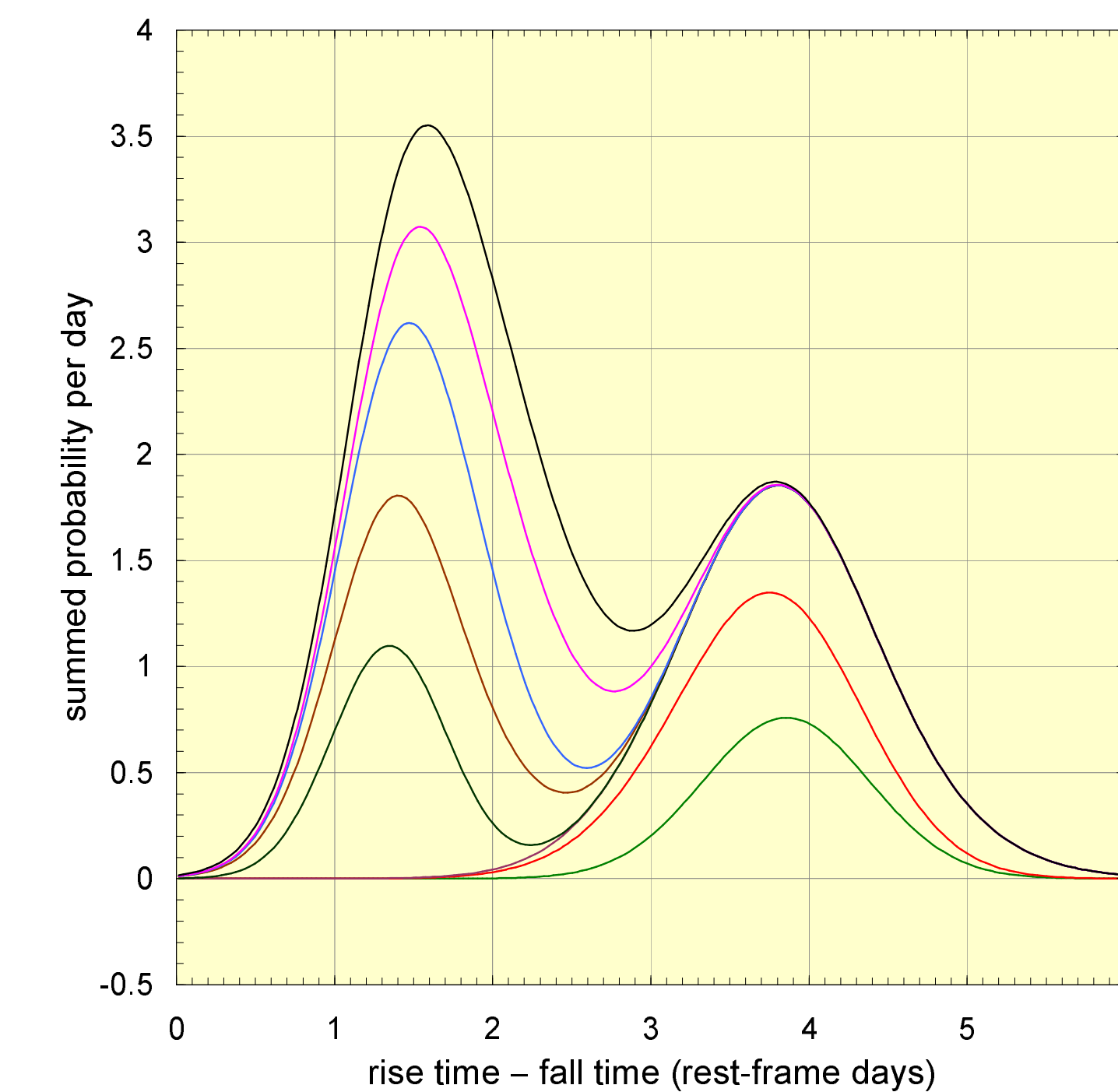


FIG. 4.— Ideogram showing the summed probability density function for the difference between rise time and fall time, based on the data in Fig. 3(a).

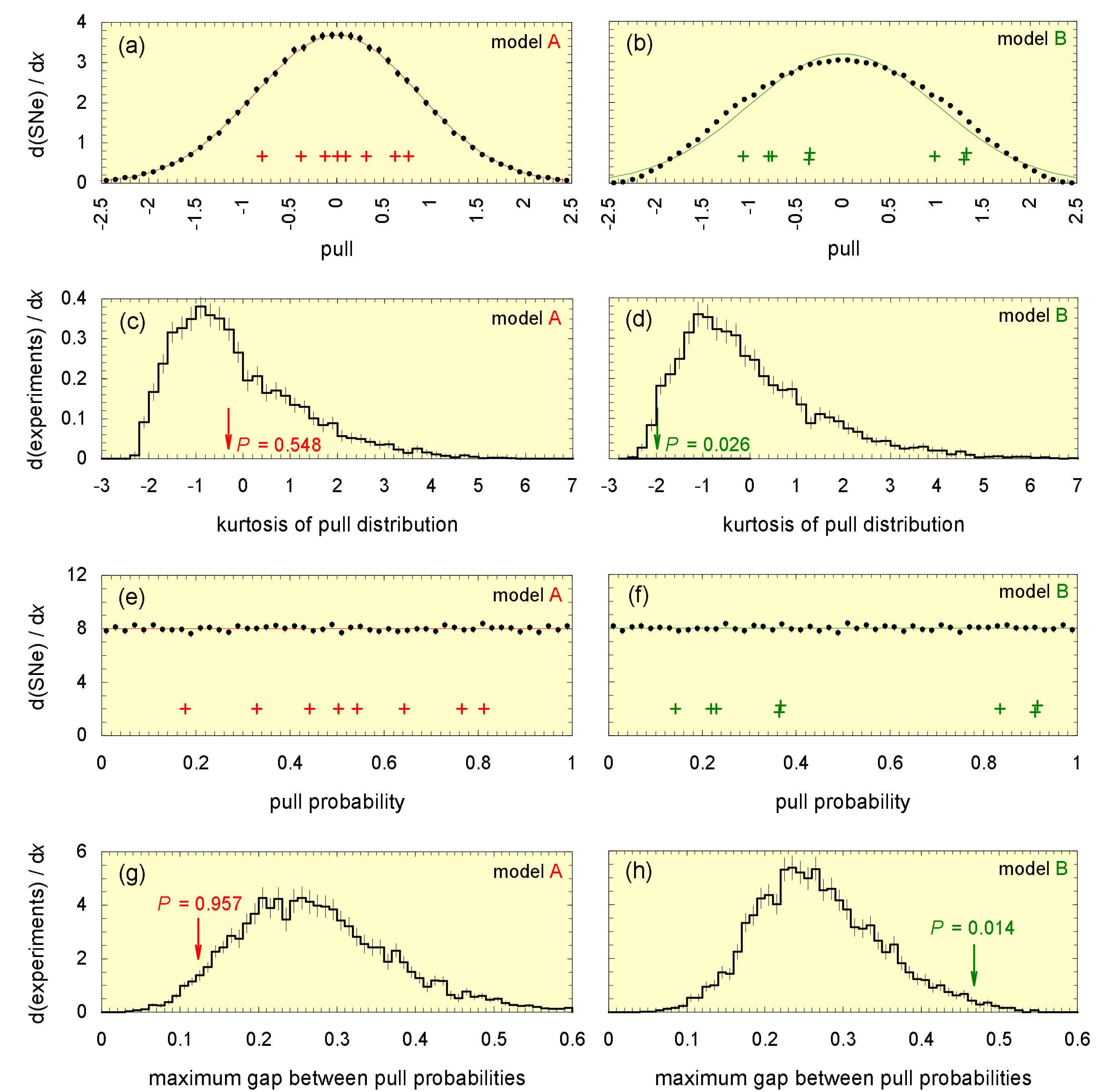


FIG. 5.— Comparison to gaussian expectation of the distribution of pulls (residuals normalized to their uncertainties) for the fits shown in Figs. 3(a) (left column) and 3(b) (right column). (a)-(b) Distribution of pulls for eight actual SNe (crosses) and for fits to eight simulated SNe (points). The gaussian curve has the same rms as the points. (c)-(d) Kurtosis of the pull distribution for eight actual SNe (arrow) and for sets of eight simulated SNe (histogram). (e)-(f) Same as (a)-(b) except that the pull is mapped to a function (“pull probability”) that is distributed uniformly on (0,1). (g)-(h) Distribution of the maximum interval in pull probability between neighboring interior SNe, for eight actual SNe (arrow) and for sets of eight simulated SNe (histogram).